Identification of Candidate Substrates for the Golgi Tul1 E3 Ligase Using Quantitative diGly Proteomics in Yeast*[S]

Zongtian Tong‡, Min-Sik Kim§, Akhilesh Pandey§¶‖, and Peter J. Espenshade‡‡‡**

Maintenance of protein homeostasis is essential for cellular survival. Central to this regulation are mechanisms of protein quality control in which misfolded proteins are recognized and degraded by the ubiquitin-proteasome system. One well-studied protein quality control pathway requires endoplasmic reticulum (ER)-resident, multi-subunit E3 ubiquitin ligases that function in ER-associated degradation. Using fission yeast, our lab identified the Golgi Dsc E3 ligase as required for proteolytic activation of fungal sterol regulatory element-binding protein transcription factors. The Dsc E3 ligase contains five integral membrane subunits and structurally resembles ER-associated degradation E3 ligases. *Saccharomyces cerevisiae* codes for homologs of Dsc E3 ligase subunits, including the Dsc1 E3 ligase homolog Tul1 that functions in Golgi protein quality control. Interestingly, *S. cerevisiae* lacks sterol regulatory element-binding protein homologs, indicating that novel Tul1 E3 ligase substrates exist.

Here, we show that the *S. cerevisiae* Tul1 E3 ligase consists of Tul1, Dsc2, Dsc3, and Ubx3 and define Tul1 complex architecture. Tul1 E3 ligase function required each subunit as judged by vacuolar sorting of the artificial substrate Pep12D. Genetic studies demonstrated that Tul1 E3 ligase was required in cells lacking the multivesicular body pathway and under conditions of ubiquitin depletion. To identify candidate substrates, we performed quantitative diGly proteomics using stable isotope labeling by amino acids in cell culture to survey ubiquitylation in wild-type and *tul1*Δ cells. We identified 3116 non-redundant ubiquitylation sites, including 10 sites in candidate substrates. Quantitative proteomics found 4.5% of quantified proteins (53/1172) to be differentially expressed in *tul1*Δ cells. Correcting the diGly dataset for these differences increased the number of Tul1-dependent ubiquitylation sites. Together, our data demonstrate that the Tul1 E3 ligase functions in protein homeostasis under non-stress conditions and support a role in protein quality control. This quantitative diGly proteomics methodology will serve as a robust platform for screening for stress conditions that require Tul1 E3 ligase activity. ***Molecular & Cellular Proteomics 13: 10.1074/mcp.M114.040774, 2871–2882, 2014.***

Control of protein homeostasis or proteostasis is key for cell function and survival (1). An important aspect of proteostasis is protein quality control in which misfolded proteins are recognized and degraded by the ubiquitin-proteasome pathway (2). Complex mechanisms regulate whether proteins are targeted for degradation, but ultimately misfolded proteins are recognized and ubiquitylated by specific E2 ubiquitin-conjugating enzymes and E3 ubiquitin ligases (3). One well-studied protein quality control pathway is ER-associated degradation (ERAD)[1] (4–6). ER luminal and membrane proteins are targeted for cytosolic proteasomal degradation by a set of multisubunit E3 ligases integral to the ER membrane, such as Hrd1 and Doa10 in *Saccharomyces cerevisiae* and Hrd1 and gp78 in mammals. Key open questions in the protein quality control field are (i) what are the physiological substrates of protein quality control pathways and (ii) how do these E3 ligases recognize proteins for degradation.

The sterol regulatory element–binding protein (SREBP) family of transcription factors regulates lipid homeostasis in mammals and fungi (7). These ER membrane-bound proteins are proteolytically activated in the Golgi to release the transcription factor domain from the membrane, allowing it to

From the ‡Department of Cell Biology, Johns Hopkins University School of Medicine, Baltimore, Maryland 21205; §McKusick-Nathans Institute of Genetic Medicine, Johns Hopkins University School of Medicine, Baltimore, Maryland 21205; ¶Departments of Biological Chemistry, Oncology and Pathology, Johns Hopkins University School of Medicine, Baltimore, Maryland 21205; ‖Adrienne Helis Malvin Medical Research Foundation, New Orleans, Louisiana 70130; **Diana Helis Henry Medical Research Foundation, New Orleans, Louisiana 70130

Received May 1, 2014, and in revised form, July 30, 2014

Published, MCP Papers in Press, July 30, 2014, DOI 10.1074/mcp.M114.040774

Author contributions: Z.T., M.K., A.P., and P.J.E. designed research; Z.T. and M.K. performed research; Z.T. contributed new reagents or analytic tools; Z.T., M.K., A.P., and P.J.E. analyzed data; Z.T., M.K., A.P., and P.J.E. wrote the paper.

[1] The abbreviations used are: ERAD, endoplasmic reticulum–associated degradation; ER, endoplasmic reticulum; SREBP, sterol regulatory element–binding protein; Dsc, defective for SREBP cleavage; SNARE, soluble NSF attachment protein receptor; MVB, multivesicular body; MS, mass spectrometry; SILAC, stable isotope labeling by amino acids in cell culture; Ni-NTA, nickel-nitrilotriacetic acid; TFA, trifluoroacetic acid; ACN, acetonitrile; FA, formic acid; ESCRT, endosomal sorting complex required for transport; H/L, heavy-to-light.

activate gene expression. Studies of the SREBP pathway in the fission yeast *Schizosaccharomyces pombe* led to the discovery of the Golgi Dsc E3 ligase that is required for the cleavage of yeast SREBPs (8, 9). The Golgi Dsc E3 ligase contains five subunits, Dsc1–Dsc5, that form a stable complex with a defined architecture (10). Dsc1 is a really interesting new gene (RING) domain-containing E3 ubiquitin ligase, and its RING domain function is required for SREBP cleavage (8, 11). Collectively, data are consistent with SREBPs being substrates for the Dsc E3 ligase, but ubiquitylation has not been demonstrated. Interestingly, the subunits and organization of the Dsc E3 ligase resemble the Hrd1 and gp78 E3 ligases that function in ERAD (10, 12). This similarity to ERAD E3 ligases, along with the Golgi localization, suggests a broader role for the Dsc E3 ligase in Golgi protein quality control and degradation.

The budding yeast *S. cerevisiae* encodes sequence homologs of Dsc E3 ligase subunits, but *S. cerevisiae* lacks SREBPs, suggesting that additional substrates exist for this Golgi enzyme. We reasoned that characterizing the function of the Dsc E3 ligase in *S. cerevisiae* would advance our understanding of its role in Golgi protein degradation outside of the SREBP pathway. To date, only *S. cerevisiae* Tul1, the homolog of *S. pombe* Dsc1, has been characterized in detail. Tul1 is an integral Golgi membrane protein with a carboxy-terminal RING domain that binds and functions with the E2 ubiquitin-conjugating enzyme Ubc4 (13). Tul1 functions in Golgi protein quality control insomuch as Tul1 ubiquitylates Pep12D, a mutant endosomal SNARE protein with a transmembrane domain containing a charged residue (13). As a consequence of ubiquitylation, Pep12D is sorted into the multivesicular body (MVB) pathway that results in vacuolar degradation rather than localizing to the limiting membrane of the vacuole. In addition, Tul1 recognizes unpalmitoylated SNARE Tlg1 and targets this mutant protein to the MVB pathway (14). Although Tul1 acts on these engineered mutant proteins, no endogenous physiological substrates have been identified.

Stable isotope labeling by amino acids in cell culture (SILAC) is a well-established method for labeling the cellular proteome to allow precise mass spectrometry (MS)-based protein quantitation (15–17). Recent technical advances enable enrichment of ubiquitylated peptides and greatly improve detection of this post-translational modification (18). Antibodies that recognize the diGly remnant on ubiquitin-conjugated lysine residues after trypsin digestion now allow the identification of thousands of ubiquitylated peptides via MS (19–21). Combining these tools permits quantitative analysis of ubiquitylation sites under different experimental conditions (20–26).

In this study, we characterized the *S. cerevisiae* Tul1 E3 ligase complex. Here we define its subunit architecture and demonstrate that all four subunits are required for Tul1 function in Golgi protein quality control. Genetic studies indicate that Tul1 function is required in the absence of the MVB degradation pathway and under conditions of ubiquitin depletion. We used quantitative diGly proteomics to identify 3116 ubiquitylation sites in *S. cerevisiae* and found 10 candidate Tul1 E3 ligase substrates. Quantitative proteomics in wild-type and *tul1*Δ cells revealed that Tul1 functions in proteostasis under non-stress conditions. Collectively, these data are consistent with the proposed function for the Tul1 E3 ligase in Golgi protein quality control.

EXPERIMENTAL PROCEDURES

Yeast Strains, Plasmids, and Media—*S. cerevisiae* BY4741-derived strains (S288C background, supplemental Table S1) were generated using homologous recombination and standard molecular biology and genetic techniques (27, 28). Yeast strains were cultured in rich yeast extract peptone dextrose medium in exponential phase unless otherwise noted. Geneticin (100 μg/l, Invitrogen) and ClonNAT (100 μg/l, Werner, BioAgents, Jena, Germany) were used to select for the *kanMX* and *natMX* marker genes, respectively. Plasmids pUB221 [P_{CUP1}-6HIS-myc-ubiquitin, 2μ, *URA3*], pUB100 [*ubi1*-tail, CEN, *HIS3*], and GFP-Pep12D [P_{TPI1}-GFP-Pep12D, CEN, *URA3*] were described previously (13, 29, 30).

Antibody Preparation and Immunoblotting—Hexahistidine-tagged recombinant protein antigens, Tul1 (amino acids 31–300), Dsc2 (amino acids 241–322), Dsc3 (amino acids 35–185), and Ubx3 (amino acids 265–455), were purified from *Escherichia coli* using Ni-NTA (Qiagen, Valencia, CA) according to the manufacturer's instructions. Tul1, Dsc3, Dsc3, and Ubx3 antisera were generated by Covance Inc. using a standard protocol. Affinity-purified antibodies (anti-Dsc IgG) were isolated from rabbit antisera via affinity chromatography using Tul1, Dsc2, Dsc3, and Ubx3 antigens and the AminoLink Plus Immobilization Kit (Pierce) according to the manufacturer's instructions. Affinity-purified anti-Tul1-HRP, anti-Dsc2-HRP, anti-Dsc3-HRP, and anti-Ubx3-HRP were generated using an EZ-Link Plus Activated Peroxidase kit (Pierce). Microsome preparation and immunoblotting was performed as described previously (8). PNGaseF treatment of microsomal extracts was performed according to the manufacturer's instructions (New England Biolabs, Ipswich, MA).

Co-immunoprecipitation—Exponentially growing cells (5×10^8 cells) were washed with water and resuspended in 500 μl of immunoprecipitation buffer (50 mM HEPES-KOH, pH 6.8, 150 mM KOAc, 2 mM MgOAc, 1 mM $CaCl_2$, 15% glycerol) with 0.1% digitonin and supplemented with 1× Complete Protease Inhibitor - EDTA (Roche). Cell lysates were prepared by bead-beating (0.5 mm, Sigma) at 4 °C followed by the addition of 500 μl of immunoprecipitation buffer with 1.9% digitonin to raise the final digitonin concentration to 1%. Membrane proteins were solubilized by rotating lysates at 4 °C for 40 min. Non-solubilized material was removed by centrifugation at 100,000*g* for 10 min, and an equal amount of clarified lysates (1 mg of total protein in a 1-ml volume) was incubated with affinity-purified anti-Dsc2, anti-Dsc3, or anti-Ubx3 IgG (30 μg) for 2 h. Incubation was followed by the addition of 20 μl of recombinant protein A affinity resin (Repligen, Waltham, MA) and overnight incubation. Protein A affinity resin was then washed four times with 1 ml of immunoprecipitation buffer containing 0.1% digitonin, and bound proteins were eluted by boiling with 100 μl of SDS lysis buffer (31). Equal amounts of total and unbound fractions were immunoblotted along with 5× bound fractions.

Real-time PCR—Total RNA was isolated, and first-strand cDNA was synthesized as described previously (32). cDNA was quantified via real-time PCR using GoTaq qPCR Master Mix (Promega, Madison WI) and a MyiQ single-color-detection thermal cycler (Bio-Rad). Each sample was analyzed in triplicate using gene-specific primers chosen

using Primer3 software to amplify a ~100-bp fragment upstream of the stop codon.

Fluorescence Microscopy—Cells were observed using a Zeiss Axioskop microscope equipped with fluorescence and Nomarski optics (Zeiss, Thornwood, NY). Images were captured with a Photometrics Cool Snap EZ CCD camera and IP Lab Spectrum software (Biovision Technologies, Inc., Exton, PA). GFP images were processed using Image J software (NIH).

Quantitative Proteomic Analysis by SILAC—Wild-type (JMP001) and *tul1*Δ strain (PEY1619) were cultured for approximately eight generations to reach A_{600} of 1.0 in 500 ml of Synthetic Complete medium lacking lysine (33) that was supplemented with L-lysine (30 mg/l) and an equal molar amount of $^{13}C_6{}^{15}N_2$ L-lysine (+8.0142 Da, Cambridge Isotope Laboratories, Tewksbury, MA) for light and heavy media, respectively. Differentially labeled cells were lysed separately in buffer A (10 mM Tris-HCl, pH 8.0, 100 mM NaH_2PO_4, 8 M urea, 10 mM β-mercaptoethanol) using Avestin Emulsiflex C3 homogenizer. Clarified cell lysates were mixed 1:1 based on their protein content (250 mg total) and then loaded onto an Ni-NTA column (1.5-ml packed volume). After a wash with buffer A, ubiquitylated proteins were eluted using the elution buffer (8 M urea, 10 mM Tris, 100 mM sodium phosphate, pH 4.5) as described (34).

Peptide Preparation—Ubiquitylated proteins in elution buffer were exchanged to high-pH urea buffer (8 M urea, 20 mM HEPES, pH 8.0), and a total of 4.1 μg and 3.8 μg of enriched ubiquitylated proteins from biological replicates were reduced with 5 mM dithiothreitol for 30 min at 60 °C, subsequently cooled down on ice, and alkylated using 10 mM iodoacetamide for 30 min at room temperature in the dark. Lysates were then diluted to 2 M urea with 20 mM HEPES, pH 8.0, and digested overnight at room temperature with trypsin (Worthington) at an enzyme-to-substrate ratio of 1:25 (w/w). Tryptic digestion efficiency was assessed via SDS-PAGE prior to processing. A mixture of tryptic peptide samples was acidified with trifluoroacetic acid (TFA) to a final concentration of 1% and subsequently desalted using a C_{18} Sep-Pak SPE cartridge (Waters, Milford, MA). C_{18} cartridges were conditioned with 3 ml of 80% acetonitrile (ACN) followed by 3 ml of 50% ACN (0.1% TFA), and finally 5 ml of 0.1% TFA. Digest samples were loaded onto the conditioned C_{18} cartridge, washed with 2 ml of 0.1% TFA three times, and eluted with 2 ml of 50% ACN (0.1% TFA) twice. Eluates were lyophilized at −80 °C for 2 days.

For whole proteome analysis, equal amounts of proteins extracted from both wild-type and *tul1*Δ strains were mixed (70 μg total), and two biological replicates of mixed samples were separated via SDS-PAGE using a gradient gel (4–12% NuPAGE® Bis-Tris Precast Gel, Novex, Invitrogen). A total of 18 gel slices were excised from the replicate samples, and proteins in the gel slices were digested by lysyl endopeptidase (Wako, Richmond, VA) after reduction by dithiothreitol and alkylation by iodoacetamide (35). Peptides extracted with 50% acetonitrile (0.1% formic acid) were vacuum-dried and kept at −20 °C until LC-MS/MS analysis.

K-ε-GG Peptide Enrichment—Anti-K-ε-GG antibody was obtained as part of the PTMScan ubiquitin remnant motif (K-ε-GG) kit (Cell Signaling Technology, Danvers, MA). Immunoaffinity purification of ubiquitylated peptides was carried out per the manufacturer's instructions. In brief, lyophilized peptides were resuspended in 1.5 ml of ice-cold immunoprecipitation buffer (IAP) (50 mM MOPS, pH 7.2, 10 mM sodium phosphate, 50 mM NaCl) and incubated for 30 min with preincubated anti-K-ε-GG antibody beads in the IAP buffer on a rotator at 4 °C. Anti-K-ε-GG antibody beads were washed with 1 ml of cold IAP buffer twice and 1 ml of cold H_2O three times prior to elution of enriched ubiquitylated peptides with 40 μl of 0.15% TFA solution twice. Eluted peptide supernatants were desalted using C_{18} STAGE tips (36). STAGE tips were packed with a C_{18} Empore disk 3M, St. Paul, MN and conditioned with 100 μl of 80% ACN (0.1% formic acid (FA)), 100 μl of 50% ACN (0.1% FA), and two applications of 100 μl of 0.1% FA before the peptide solution was loaded. Peptides were washed twice with 100 μl of 0.1% FA and eluted with 50 μl of 50% ACN (0.1% FA). Desalted peptides were dried and kept at −20 °C in a freezer until LC-MS/MS analysis.

LC-MS/MS Analysis—Dry peptides were resuspended in 9 μl of 0.1% FA, out of which 8 μl of peptide solution was loaded onto a trap column (2 cm long × 360 μm outer diameter × 75 μm inner diameter) and separated by an analytical column (20 cm long × 360 μm outer diameter × 75 μm inner diameter) packed in-house with C_{18} packing material (Magic C18 AQ, 3-μm size, 100-Å pore). Solvent A was 0.1% FA, and solvent B was 90% ACN (0.1% FA). Peptides were resolved with a solvent gradient generated by a Proxeon Easy-nLC system coupled online to an LTQ-Orbitrap Elite mass spectrometer. Peptides eluted were ionized by the nano-electrospray ionization at 1.8 kV, and peptide ions were introduced directly into the mass spectrometer at a flow rate of 300 nl/min of solvent with a gradient of 8% B for 1 min, 35% B for 115 min, 95% for 14 min, and 95% for 20 min with a total running time of 150 min. The mass spectrometer was operated in data-dependent acquisition mode acquiring higher-energy collisional dissociation MS/MS scans (r = 30,000) after each precursor scan (r = 120,000) on the 15 most abundant ions using an MS1 target of 1×10^6 ions and an MS/MS target of 5×10^4 ions. The maximum ion time used for MS/MS scans was 300 ms, the higher-energy collisional dissociation normalized collision energy was set at 32%, and the dynamic exclusion time was set at 60 s. For the whole proteome analysis, all the parameters were identical except for the nano-electrospray ionization at 2.0 kV and a total running time of 100 min.

Mass Spectrometry Data Analysis—Mass spectrometry data were analyzed using the MaxQuant platform (1.3.0.5) (37) and searched against the NCBI Yeast Reference Protein Sequence database (downloaded July 2012) containing 6026 entries including 115 common laboratory contaminants provided by GPM using the Andromeda database search algorithm (38). The enzyme specificity was set to trypsin with up to two missed cleavages allowed. The "Lysine8" option was selected for a SILAC heavy label with a maximum of three labeled amino acids in a given peptide. The precursor mass tolerance was set to 20 ppm for the first search and 10 ppm for the main search. Variable modifications were set as follows: oxidation at methionine, GlyGly addition to lysine, and acetylation at protein N terminus, with a fixed modification set to carbamidomethylation at cysteine. A maximum of five modifications were allowed in a given peptide. The false discovery rates at peptide, protein, and site identification levels were set at 0.01. Ubiquitylation sites with wild-type:*tul1*Δ ratios ≥ 2.0 were manually confirmed (Table I). Site identification and quantification values were obtained from the MaxQuant GlyGly site table. Peptide ratios were normalized such that the median equaled zero. Data analysis from the whole proteome was carried out using MaxQuant (1.4.1.2) with the same protein database used in the ubiquitylated peptide analysis. The enzyme specificity was set to LysC/P with a maximum of two missed cleavages allowed. Mass errors for precursor and fragment ions were set to 7 ppm and 20 ppm, respectively. Variable modifications were set as follows: pyro-glu at glutamine, oxidation at methionine, and acetylation at protein N terminus, with a fixed modification set to carbamidomethylation at cysteine. The false discovery rates at both peptide spectrum match and protein levels were set at 0.01.

Data Availability—Mass spectrometry proteomics data have been deposited to the ProteomeXchange Consortium via the PRIDE partner repository with the dataset identifier PXD000918 (39).

RESULTS

S. cerevisiae Tul1 E3 Ligase—Bioinformatic analysis of the *S. cerevisiae* genome revealed *S. cerevisiae* homologs of Dsc

A. *S. cerevisiae DSC* Homologs

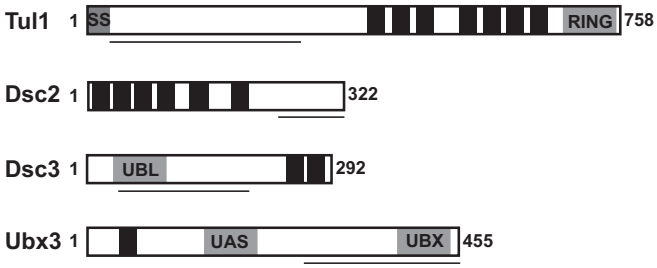

B. DRYGIN Database Correlation Coefficients

		GENE 2			
		TUL1	***DSC2***	***DSC3***	***UBX3***
GENE 1	***TUL1***		0.332	0.145	–
	DSC2	–		0.247	–
	DSC3	–	–		–
	UBX3	0.217	0.247	0.145	

FIG. 1. ***S. cerevisiae* Dsc homologs.** *A*, schematics of Dsc homologs in which black boxes represent predicted transmembrane domains. Predicted signal sequence (SS) and conserved domains are indicated. Underlining denotes amino acids used as antigens for antibody production. *B*, Pearson correlation coefficients between genetic signatures of *S. cerevisiae DSC* homologs from DRYGIN database (45). Genetic interactions were tested in a pairwise fashion such that each gene yielded two datasets. The database default setting for significance is CC $>$ 0.1, and dashes denote the absence of a correlation coefficient in database.

subunits. *S. pombe dsc1*, *dsc2*, *dsc3*, and *dsc5* correspond to *TUL1*, *YOL073C*, *YOR223W*, and *UBX3* in *S. cerevisiae* (Fig. 1*A*). We did not identify an *S. cerevisiae* homolog for *dsc4*. We named the two uncharacterized genes *YOL073C* and *YOR223W*, *DSC2* and *DSC3*, respectively (40). Tul1 is an integral membrane RING E3 ubiquitin ligase that localizes to the Golgi (13). Dsc2 is a multi-transmembrane protein with sequence similarity to Der1 and UBAC2, rhomboid pseudoproteases that function in ERAD (12, 41–43). A conserved domain search using Dsc3 identified an N-terminal ubiquitin-like domain (Fig. 1*A*). Ubx3 is predicted to contain both a UAS domain and a C-terminal UBX domain that is known to interact with the AAA-ATPase Cdc48 (44). The DRYGIN database revealed strong genetic correlations among *TUL1*, *DSC2*, *DSC3*, and *UBX3*, suggesting that these genes function in a related process (Fig. 1*B*) (45). In addition, comparisons of genetic interactions between *S. pombe* and *S. cerevisiae* suggested that these four proteins form a complex, and we confirmed this biochemically (40). Collectively, these data demonstrate that Tul1, Dsc2, Dsc3, and Ubx3 are subunits of the Tul1 E3 ligase in *S. cerevisiae* that is homologous to the *S. pombe* Dsc E3 ligase.

To further characterize the Tul1 E3 ligase, we analyzed protein levels in the absence of individual subunits. Tul1 was reduced in *dsc2*Δ, *dsc3*Δ, and *ubx3*Δ cells (Fig. 2*A*). Dsc3 was slightly reduced in *dsc2*Δ and *ubx3*Δ cells, but not in *tul1*Δ cells. Expression of Dsc2 and Ubx3 was unchanged in the mutants. Treatment of microsomal extracts with the glycosidase PNGaseF increased the mobility of Tul1, demonstrating that Tul1 is N-glycosylated (Fig. 2*B*). In line with this, the N terminus of Tul1 contains eight potential *N*-linked glycosylation sites and is predicted to localize to the secretory pathway lumen. Parallel analysis of Dsc2, Dsc3, and Ubx3 showed no changes in protein mobility (data not shown). Treatment of microsomal extracts with phosphatase had no effect on the mobility of Tul1, Dsc2, Dsc3, and Ubx3, indicating that these proteins are not highly phosphorylated (data not shown). Thus, Tul1 is a glycoprotein whose expression in wild-type cells requires each subunit of the Tul1 E3 ligase.

Quantitative real-time PCR analysis showed no significant change in *TUL1* mRNA between wild-type and mutant cells, indicating that *TUL1* transcription was not altered (supplemental Fig. S1). Treatment of wild-type and mutant cells with the proteasome inhibitor MG-132 had no effect on Tul1 expression (Fig. 2*C*) but increased expression of Dsc3 in *dsc2*Δ and *ubx3*Δ cells, suggesting that Dsc3 is degraded by the proteasome in the absence of Dsc2 or Ubx3. The yeast vacuole is another principal site of protein degradation, so we assayed Tul1 levels in vacuolar protease-deficient *pep4*Δ cells. Deletion of *PEP4* in *dsc2*Δ, *dsc3*Δ, and *ubx3*Δ cells restored Tul1 to wild-type levels but did not increase Dsc3 (Fig. 2*D*). Thus in the absence of any one E3 ligase subunit, Tul1 is degraded in a vacuole-dependent manner, whereas Dsc3 is degraded in a proteasome-dependent manner in *dsc2*Δ and *ubx3*Δ cells.

Tul1 E3 Ligase Consists of Subcomplexes—Dsc2 binds to Tul1, Dsc3, and Ubx3 when purified from detergent cell extracts (40). To confirm that these proteins constitute a single complex and to probe its architecture, we performed co-immunoprecipitation analysis for each subunit and tested the requirement of individual subunits for complex assembly. We pulled down endogenous Dsc2, Dsc3, and Ubx3 from digitonin-solubilized cell extracts and subjected them to immunoblot analysis with HRP-conjugated antibodies against Tul1, Dsc2, Dsc3, and Ubx3. We were unable to functionally epitope-tag Tul1, and Tul1 antiserum did not function for immunoprecipitation. Protein antigens are described in Fig. 1. Antibodies to Dsc2, Dsc3, and Ubx3 recovered a complex from wild-type cells that contained the four subunits (Figs. 3*A*–3*C*, lane 6), demonstrating that Tul1, Dsc2, Dsc3, and Ubx3 form a multi-subunit E3 ligase complex.

To probe complex architecture, we performed co-immunoprecipitation in subunit mutants. Dsc2 and Ubx3 formed a subcomplex in the absence of either Tul1 or Dsc3 (Figs. 3*A* and 3*C*, lanes 7 and 9). Dsc3 formed a subcomplex with Dsc2-Ubx3 that did not require Tul1 (Figs. 3*A*–3*C*, lane 7), but deletion of either *DSC2* or *UBX3* disrupted Dsc3 binding to the other subunits (Fig. 3*B*, lanes 8 and 10). Binding of Tul1 to any subunit required the presence of all three other subunits (Figs. 3*A*–3*C*, lanes 6–10). These data demonstrate that the Tul1 E3 ligase consists of two subcomplexes, Dsc2-Ubx3 and

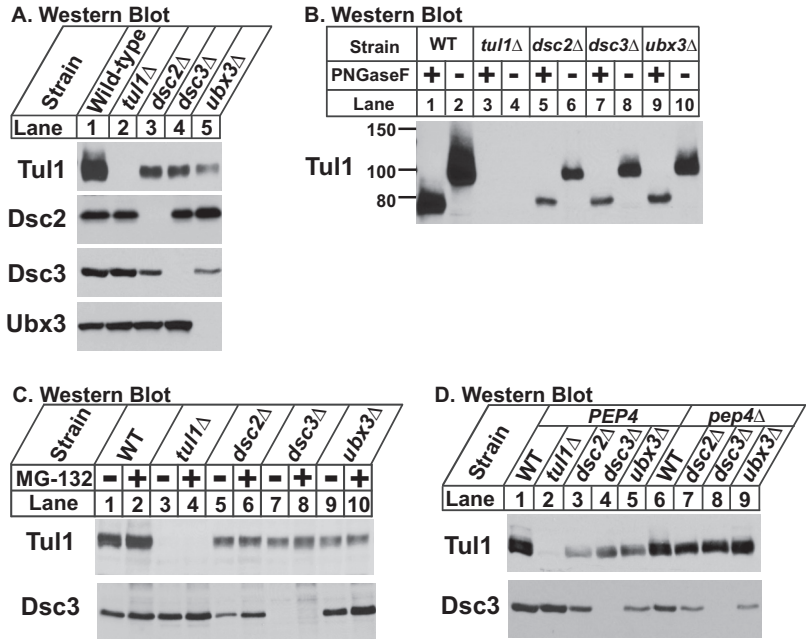

FIG. 2. **Tul1 and Dsc3 expression requires E3 ligase subunits.** *A*, microsomal extracts from wild-type, *tul1*Δ, *dsc2*Δ, *dsc3*Δ, and *ubx3*Δ cells immunoblotted with anti-Tul1, anti-Dsc2, anti-Dsc3, and anti-Ubx3 IgG. *B*, microsomal extracts from wild-type, *tul1*Δ, *dsc2*Δ, *dsc3*Δ, and *ubx3*Δ cells were treated in the presence or absence of PNGase F and immunoblotted with anti-Tul1 IgG. *C*, indicated strains were treated with proteasome inhibitor MG-132 (100 μM) or dimethyl sulfoxide for 2 h. Microsomal extracts were prepared and immunoblotted with anti-Tul1 and anti-Dsc3 IgG. *D*, microsomal extracts from the indicated strains were prepared and immunoblotted with anti-Tul1 and anti-Dsc3 IgG.

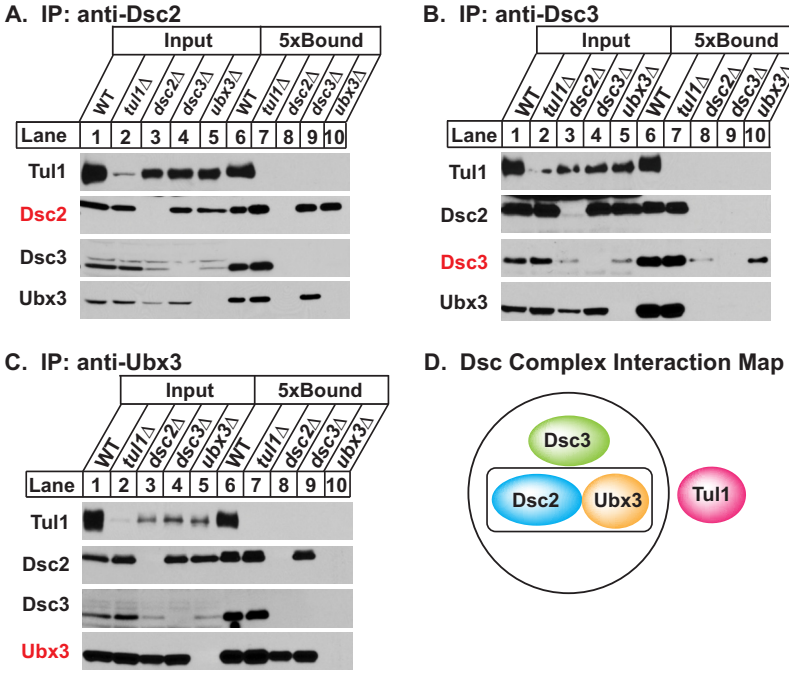

FIG. 3. **Tul1 E3 ligase subunits form distinct subcomplexes.** *A*, digitonin-solubilized extracts from wild-type, *tul1*Δ, *dsc2*Δ, *dsc3*Δ, and *ubx3*Δ cells were prepared, and proteins associated with Dsc2 were immunopurified by anti-Dsc2 affinity-purified antibodies. Equal amounts of input and 5× bound fractions were immunoblotted using HRP-conjugated anti-Tul1, anti-Dsc2, anti-Dsc3, and anti-Ubx3 antibodies. *B*, *C*, proteins associated with Dsc3 or Ubx3, respectively, were immunopurified as described in *A* using anti-Dsc3 or anti-Ubx3 affinity-purified antibodies. Equal amounts of input and 5× bound fractions were immunoblotted using HRP-conjugated anti-Tul1, anti-Dsc2, anti-Dsc3, and anti-Ubx3 antibodies. *D*, model illustrating the results from co-immunoprecipitation experiments in *A*–*C*. Complexes and subcomplexes observed in wild-type and mutant cells are indicated. Contacts do not denote direct protein–protein interactions.

Dsc2-Ubx3-Dsc3 (Fig. 3*D*), and that Tul1 binding to the complex occurs only once the Dsc2-Ubx3-Dsc3 subcomplex has assembled. These data are completely consistent with the genetic requirements for protein expression in Fig. 2, suggesting that the reduced expression of Tul1 and Dsc3 resulted from failure to assemble Tul1 E3 ligase subcomplexes.

Pep12D Vacuolar Sorting Requires the Tul1 E3 Ligase—The endosomal SNARE Pep12 localizes primarily to late endo-

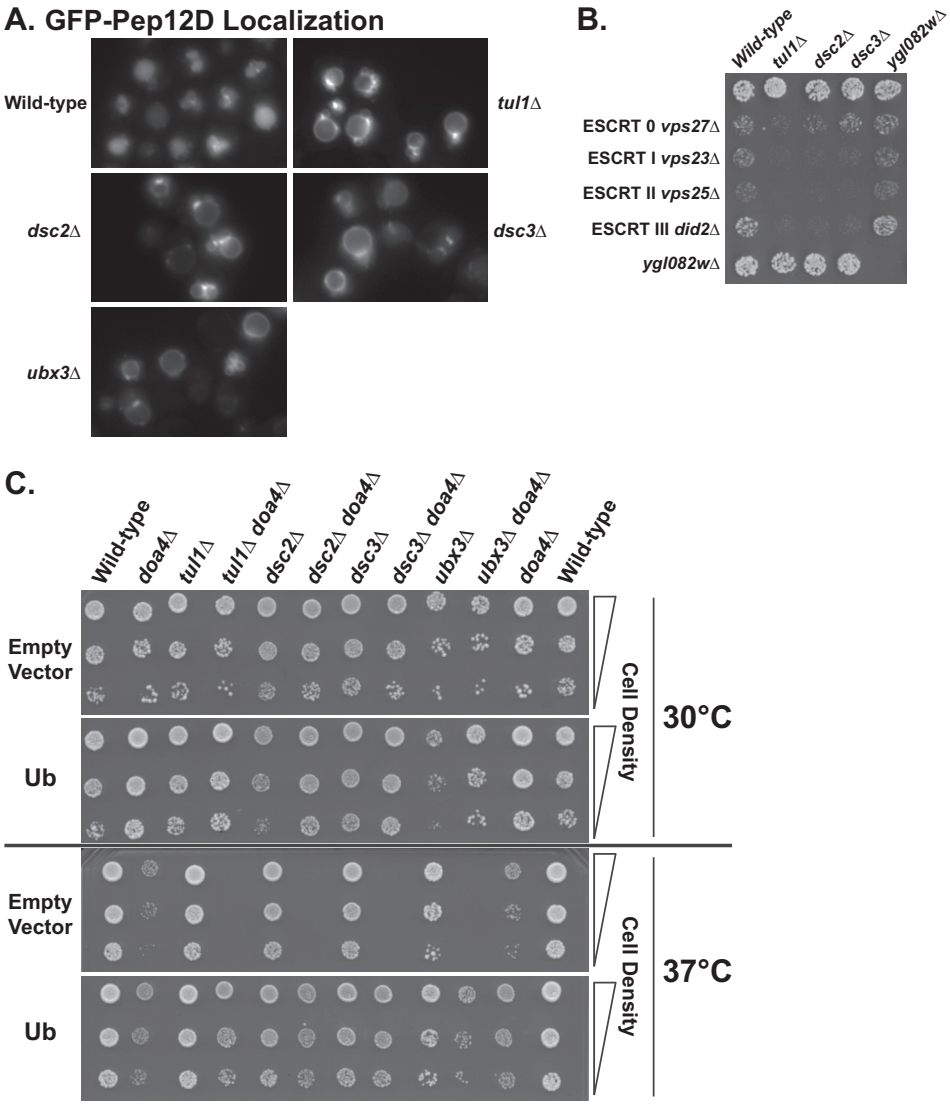

FIG. 4. **Tul1 E3 ligase complex displays genetic interactions with the multivesicular body pathway.** *A*, indicated strains expressing GFP-tagged mutant form of Pep12 (Pep12D) were imaged using fluorescence microscopy. Staining of vacuolar lumen or limiting membrane is visible. *B*, indicated single and double mutant yeast strains were spotted on YPD rich medium at 37 °C and grown for 2 days. *C*, 5-fold serial dilutions of indicated single and double mutants carrying empty vector (pRS426) or expressing 6HIS-myc-ubiquitin (pUB221) were spotted on YPD rich medium with no added copper at 30 °C or 37 °C and grown for 2 days.

somes, but when overexpressed it localizes to the limiting membrane of the vacuole (46, 47). Mutant Pep12 that contains a single aspartic acid residue in its transmembrane domain (GFP-Pep12D) is sorted through the MVB pathway to the vacuolar lumen where the GFP tag accumulates (48). Sorting to the vacuolar lumen requires Tul1-dependent ubiquitylation of GFP-Pep12D (13). To test whether other subunits of the Tul1 E3 ligase are required for sorting Pep12D into the vacuolar lumen, we examined the localization of GFP-Pep12D in mutant strains. As expected, GFP-Pep12D localized to the vacuolar lumen in wild-type cells (Fig. 4*A*). Efficient luminal sorting required *TUL1* as GFP-Pep12D accumulated on the limiting membrane of the vacuole in *tul1*Δ cells (Fig. 4*A*). Deletion of *DSC2*, *DSC3*, or *UBX3* also caused GFP-Pep12D to accumulate on the vacuolar rim, indicating that these genes are also required for GFP-Pep12D ubiquitylation and proper targeting to the vacuolar lumen (Fig. 4*A*). Dsc2, Dsc3, and Ubx3 might not function directly in GFP-Pep12D ubiquitylation, as Tul1 expression was reduced in these mutants (Fig. 2*A*). These data demonstrate that Tul1, Dsc2, Dsc3, and Ubx3 form a functional E3 ligase complex required for Pep12D ubiquitylation in cells.

Tul1 E3 Ligase Subunit Genes Show Genetic Interactions with MVB Pathway Genes—The MVB pathway delivers cargo to the vacuole for degradation, and this process requires the sequential function of endosomal sorting complex required for transport (ESCRT) complexes 0, I, II, and III (49). Genetic interaction mapping in *S. pombe* revealed that genes showing

aggravating genetic interactions with *dsc1-dsc4* were highly enriched for components of the MVB pathway (8). Independently, ESCRT mutants show aggravating genetic interactions with *TUL1*, *DSC2*, *DSC3*, and *UBX3* in *S. cerevisiae* (45). To confirm the genetic interactions between Tul1 E3 ligase subunit genes and ESCRT genes, we compared the fitness of double mutants to that of the corresponding single mutants. We observed fitness defects at 37 °C for double deletion mutants of the Tul1 ligase subunit genes and genes coding for components of ESCRT I, II, III, and, to a lesser extent, 0 (Fig. 4*B*). Given that SREBP homologs are absent from *S. cerevisiae*, these data suggest that the *S. cerevisiae* Tul1 E3 ligase functions in a pathway parallel to the MVB pathway.

The ubiquitin-specific hydrolase Doa4 is also required for MVB pathway function (49). Doa4 removes ubiquitin from integral membrane proteins before sorting into intraluminal vesicles of multivesicular bodies and prior to proteasomal degradation to recycle ubiquitin. Consequently, *doa4*Δ cells have reduced levels of free ubiquitin and are temperature-sensitive for growth (50). Tul1 E3 ligase mutants showed negative genetic interactions with *doa4*Δ at 37 °C but not at 30 °C (Fig. 4*C*). Double mutants of *doa4*Δ and each of the four subunit deletion mutants failed to grow at 37 °C. Overexpression of ubiquitin in these double mutants restored growth at 37 °C, indicating that the observed synthetic lethality was due to reduced levels of ubiquitin in *doa4*Δ cells. These results indicate that cells lacking the Tul1 E3 ligase require normal levels of ubiquitin for viability. Overall, the conserved negative genetic interactions between genes coding for Tul1 ligase subunits and genes involved in the MVB pathway and the ubiquitin-proteasome pathway suggest that the Tul1 E3 ligase functions in the degradation of secretory pathway proteins in *S. cerevisiae*.

Identification of Candidate Tul1 E3 Ligase Substrates—To date, Tul1 has been shown to ubiquitylate and target Pep12D to the MVB pathway (13). In addition, Tul1 targets the unpalmitoylated endosomal SNARE Tlg1 to the MVB pathway (14). The ability of Tul1 to recognize these engineered mutant proteins suggests that Tul1 functions in a protein quality control pathway, but whether the Tul1 E3 ligase ubiquitylates endogenous proteins is unknown. To identify Tul1 substrates, we employed a methodology to detect and quantify endogenous ubiquitylated peptides using mass spectrometry and SILAC with anti-K-ε-GG remnant antibody enrichment (19, 20). We quantified ubiquitylated peptides from wild-type and *tul1*Δ cells expressing 6xHis-Myc tagged ubiquitin as the sole source of ubiquitin (Fig. 5). Wild-type and *tul1*Δ cells expressing 6xHis-Myc-tagged ubiquitin were grown in heavy and light lysine, respectively. Extracted proteins were mixed equally, and ubiquitylated proteins were then affinity purified using Ni-NTA under denaturing conditions. The resulting proteins were trypsin digested and incubated with an anti-K-ε-GG remnant antibody that recognizes the diGly remnant of ubiquitin on modified lysine residues following trypsin digestion (20). Recovered peptides were quantified using LC-MS/MS.

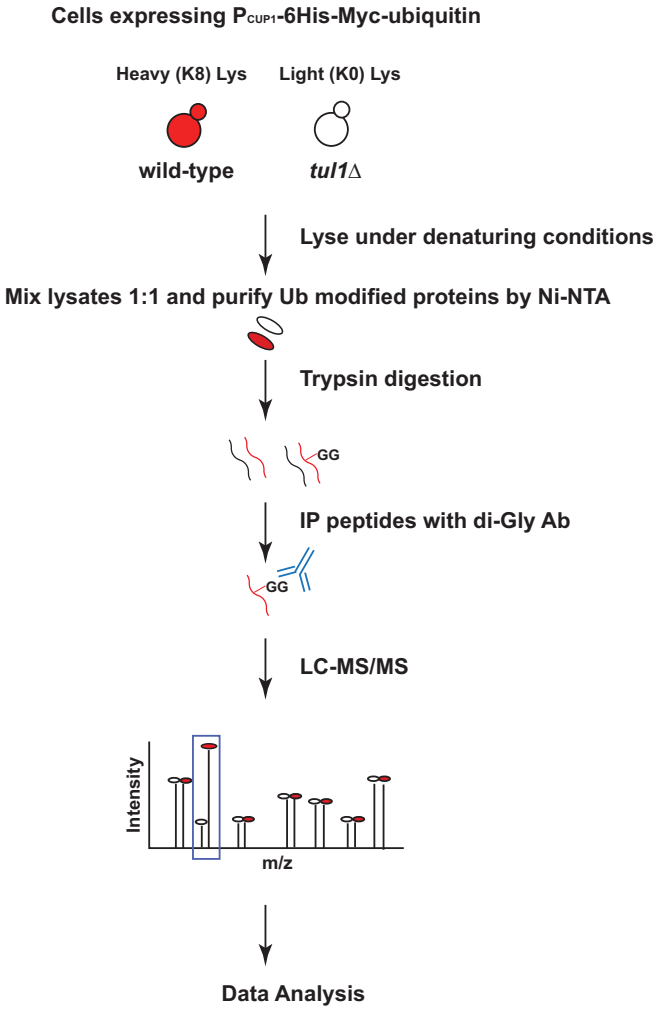

FIG. 5. **Schematic of workflow for quantification of ubiquitylated peptides.**

We performed two biological replicates using cells grown exponentially in synthetic complete medium. In total, we identified 3116 distinct K-ε-GG peptides in 1111 proteins (supplemental Table S2) and obtained a heavy-to-light (H/L) ratio in at least one experiment for 2896 ubiquitin-modified peptides (93% of the total). Multiple studies have identified ubiquitylated peptides in *S. cerevisiae*, with the recent application of quantitative diGly proteomics yielding thousands of ubiquitylated peptides per study (18, 22, 23). To evaluate our methodology, we compared our results to a published study that combined ubiquitylated protein enrichment followed by diGly proteomics without SILAC (22). We identified 25% more ubiquitylation sites (3116 compared with 2499) (Fig. 6*A*, supplemental Table S3). Interestingly, Beltrao *et al.* identified only 1221 of the sites identified in this study (39%), suggesting that many *S. cerevisiae* ubiquitylation sites remain unidentified.

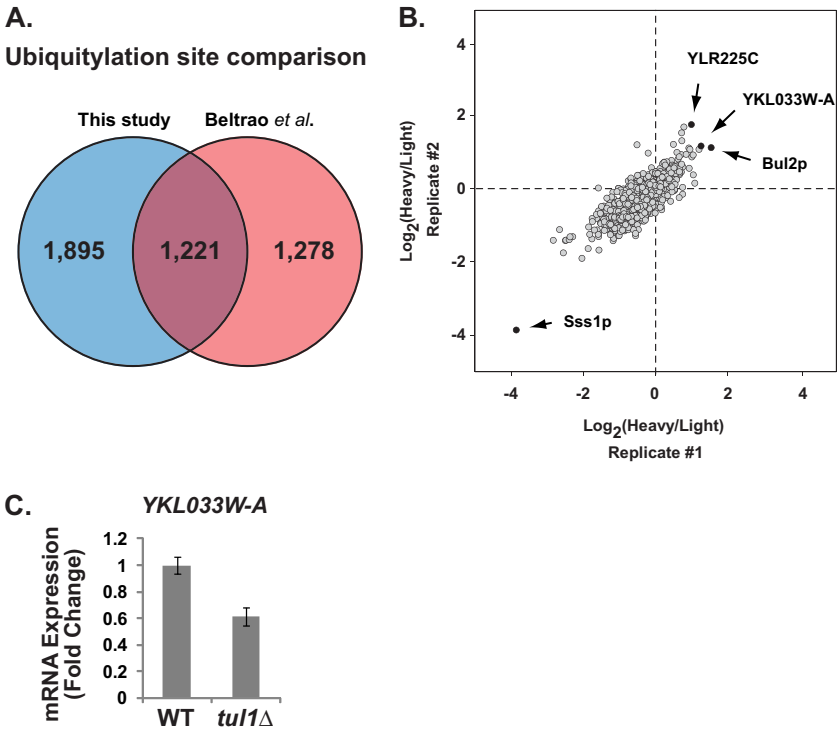

FIG. 6. **Identification of candidate Tul1 substrates using quantitative mass spectrometry.** *A*, Venn diagram comparing ubiquitylation sites found in this study and by Beltrao *et al.* (22). *B*, scatter plot of ubiquitylated peptide ratios (wild-type/*tul1*Δ) from two replicate experiments ($n = 2289$). *C*, expression of *YKL033W-A* mRNA in wild-type and *tul1*Δ cells. cDNA synthesized from total RNA (1 μg) was quantified via real-time PCR. *YKL033W-A* mRNA expression was normalized to *ACT1* and shown as fold change relative to wild-type cells. Data are the average of three biological replicates, and error bars show standard error among biological replicates.

Our use of SILAC allowed the quantification of peptide ubiquitylation between wild-type and *tul1*Δ cells. Importantly, the individual values contributing to the mean H/L ratios were highly correlated between the two replicate experiments (Fig. 6*B*). These results show that our methodology yielded reproducible quantitative data for thousands of ubiquitylated peptides. Among these data, we identified 173 peptides with differential ubiquitylation in wild-type *versus tul1*Δ cells (H/L ≥ 2.0 or H/L ≤ 0.5) (supplemental Table S4). Gene ontology searches failed to identify enrichment of particular terms ($p < 0.01$) for peptides with either increased or decreased ubiquitylation. To identify candidate Tul1 E3 ligase substrates, we reasoned that peptides from substrates would have reduced ubiquitylation in *tul1*Δ cells (H/L ≥ 2.0). Data for 10 peptides from candidate Tul1 E3 ligase substrates were manually validated and fit this criterion (Table I). Among the 10 peptides, one site was found in YKL033W-A, whose gene promoter is located immediately downstream of *TUL1* (*YKL034W*). We hypothesized that deletion of *TUL1* might affect expression of YKL033W-A, resulting in fewer YKL033W-A ubiquitylated peptides. To test this, we measured *YKL033W-A* mRNA expression in wild-type and *tul1*Δ cells via quantitative PCR. Deletion of Tul1 decreased transcription of *YKL033W-A* to 60% of that in wild-type cells (Fig. 6*C*), consistent with the reduced YKL033W-A ubiquitylation in *tul1*Δ cells. Although YKL033W-A is likely not a Tul1 E3 ligase substrate, this result validates the quality of our mass spectrometry dataset and demonstrates our ability to quantify small changes in protein ubiquitylation.

Among the other candidate substrates was Bul2, an arrestin-like adaptor and component of the Rsp5 ubiquitin ligase complex. Bul2 is itself ubiquitylated by Rsp5 (51, 52). Many yeast plasma membrane transporters and receptors are endocytosed and ultimately degraded through the MVB pathway in response to nutrient levels or signaling. Down-regulation of these proteins frequently requires arrestin ubiquitylation (53). We identified decreased ubiquitylation on Bul2 K540 in *tul1*Δ cells (Table I). In addition, we observed decreased ubiquitylation on a second residue in Bul2 K563 (H/L = 1.2, supplemental Table S5). Interestingly, we identified the corresponding residues in the homologous Bul1, but ubiquitylation was only slightly decreased in *tul1*Δ cells (H/L = 1.1 for each). Notably, Beltrao *et al.* identified these same four sites (22). These data confirm the existence of ubiquitylation sites on Bul1 and Bul2 and suggest that these residues may play a role in Rsp5-dependent regulation of plasma membrane proteins. Notably, two other arrestins, Ecm21/Art2 and Art10, are also ubiquitylated by Rsp5 (54, 55), and we detected decreased ubiquitylation of specific residues in *tul1*Δ cells (Ecm21/Art2 K95, H/L = 1.5; Art10 K118, H/L = 1.6). However, analysis of ubiquitylation for all 10 Art proteins revealed that Tul1-dependent ubiquitylation of arrestins was limited to Ecm21/Art2 and Art10 (supplemental Table S5).

To determine the role of the Tul1 E3 ligase in cellular proteostasis, we performed quantitative proteomics of whole cell lysates using SILAC. Wild-type and *tul1*Δ cells were grown in heavy and light lysine-containing media, respectively. Cell lysates were mixed, and duplicate samples were separated

TABLE I
Tul1-dependent ubiquitylation sites

Protein	Functional description	Average peptide ratio (wild type/*tul1*Δ)	Amino acid position (K)	Modified sequence
Bul2	Component of the Rsp5p E3-ubiquitin ligase complex	2.86	540	K(gl)LDQLHINNR
YLR225C	Putative protein of unknown function	2.58	22	EVLSEK(gl)DHANYTK
Akl1	Ser-Thr protein kinase of the Ark family	2.25	940	SSDASK(gl)SNQFK
YKL033W-A	Putative protein of unknown function	2.22	117	NIPIALCTSSNK(gl)TK
Aro4	3-deoxy-D-arabino-heptulosonate-7-phosphate (DAHP) synthase	2.20	136	GLINDPDVNNTFNINK(gl)GLQSAR
Zeo1	Peripheral membrane protein of the plasma membrane	2.19	81	TEAANKVEETK(gl)K
YPR084W	Putative protein of unknown function	2.17	4	(ac)SEK(gl)ASEERPIR
Rdi1	Rho GDP dissociation inhibitor	2.02	21	(ac)AEESTDFSQFEEERNNDQYK(gl)VSAK
Pal1	Protein of unknown function thought to be involved in endocytosis	2.02	291	AAPVLAFPVDGPNSTIGGASTK(gl)K
Bna1	3-hydroxyanthranilic acid dioxygenase	2.01	60	TGYHINPTPEWFYQK(gl)K

via SDS-PAGE. Proteins in gel slices were digested using LysC, and eluted peptides were quantified via LC-MS/MS. In total, we identified 1373 proteins, of which 1172 were quantified (supplemental Table S6). Of the 1373 proteins, 608 were found to be ubiquitylated proteins based on the diGly immunoprecipitation experiment (supplemental Table S7). A total of 53 proteins were found to be 2-fold differentially expressed in wild-type *versus tul1*Δ cells (40 up-regulated and 13 down-regulated; supplemental Table S8). Gene ontology searches failed to identify term enrichment ($p < 0.01$) for proteins with either increased or decreased levels between wild-type and *tul1*Δ cells. Using these data, we corrected the quantitative ubiquitylation data for differences in protein levels between the two strains (corrected values for 1823 sites; supplemental Table S9). Using this approach, we identified 196 peptides with differential ubiquitylation in wild-type *versus tul1*Δ cells ($H/L \geq 2.0$ or $H/L \leq 0.5$) (supplemental Table S10). Using the corrected values, we identified 16 additional Tul1-dependent ubiquitylation sites with $H/L \geq 2.0$ in 11 different proteins (supplemental Table S10). Overall, correcting the quantitative ubiquitylation site data for protein expression increased the number of candidate Tul1 substrates identified.

DISCUSSION

In this study, we performed a detailed characterization of the *S. cerevisiae* Golgi Tul1 E3 ligase complex. Several lines of evidence support the conclusion that Tul1, Dsc2, Dsc3, and Ubx3 form a multi-subunit E3 ligase complex that is the budding yeast equivalent of the *S. pombe* Golgi Dsc E3 ligase required for activation of SREBP transcription factors (8, 9). First, each of these proteins shows sequence homology to the fission yeast proteins, and we were able to co-purify the four subunits using antibody to Dsc2, Dsc3, and Ubx3 (Fig. 3). Second, although *S. cerevisiae* lacks a homolog of *S. pombe* Dsc4, the subunit architecture of the Tul1 E3 ligase mirrors that of the Dsc E3 ligase with Dsc2-Ubx3 forming a minimal subcomplex to which Dsc3 and Tul1 bind (10). It is possible that additional Tul1 E3 ligase subunits exist and that one of these performs the functions of Dsc4 in *S. cerevisiae*. Third, Tul1 expression requires each of the other subunits (Fig. 2*A*). Fourth, like *TUL1*, vacuolar targeting of the Pep12D mutant requires *DSC2*, *DSC3*, and *UBX3* (Fig. 4*A*). Given that Tul1 ubiquitylates Pep12D to target it to the vacuole (13), *DSC2*, *DSC3*, and *UBX3* are also likely required for Tul1 E3 ligase activity. Finally, published genetic interaction data indicate that these four genes function in the same pathway (40, 45).

Tul1 localizes to the Golgi apparatus (13), and the biochemical stability of the Tul1 E3 ligase complex suggests that the other subunits will co-localize. Tul1 is degraded in a vacuole-dependent manner in the absence of complex subunits (Fig. 2*D*). Tul1 binds to a subcomplex of Dsc2-Dsc3-Ubx3, and degradation may result from improper trafficking to the vacuole or through an autophagic pathway in the absence of complex assembly. Dsc3 binds to the Dsc2-Ubx3 subcomplex, and its protein expression requires both of these subunits (Fig. 2*A*). However, Ubx3 is degraded through a proteasome-dependent pathway (Fig. 2*C*), possibly in the endoplasmic reticulum through ERAD. These data demonstrate that the Golgi Tul1 E3 ligase consists of subcomplexes whose proper assembly is monitored by cellular quality control mechanisms.

Tul1 was identified through its ability to ubiquitylate and target the mutant Pep12D protein to the MVB pathway (13), but the physiological function of the Tul1 E3 ligase is unknown. To investigate Tul1 E3 ligase function, we sought to identify candidate substrates. We combined enrichment of ubiquitylated proteins and diGly antibody immunopurification with SILAC to perform quantitative proteomics of ubiquitin modifications in wild-type and *tul1*Δ cells (Fig. 5). We identified 3116 ubiquitylation sites and quantified 2896 of these, with results similar to those of other yeast studies employing the diGly remnant antibody (22, 23). Our methodology was sensitive, and we were able to detect a 2-fold change in the ubiquitylation of Ykl033w-a that resulted from reduced ex-

pression of this gene in *tul1*Δ cells (Fig. 6*C*). This result validates our methodology and demonstrates its ability to detect small changes in ubiquitylation.

To identify candidate Tul1 E3 ligase substrates, we focused on ubiquitylation sites whose levels changed 2-fold between wild-type and *tul1*Δ cells. Using this criterion, we identified 173 peptides with differential ubiquitylation in wild-type versus *tul1*Δ cells (supplemental Table S4). The majority of these (161 peptides) increased in *tul1*Δ cells, suggesting that they were not direct substrates of the Tul1 E3 ligase and resulted from altered physiology in *tul1*Δ cells. We expected direct Tul1 substrates to show reduced ubiquitylation in *tul1*Δ cells and validated 10 peptides as having H/L $\geq$ 2.0 (Table I). Excluding Ykl033w-a, our analysis yielded nine candidate Tul1 substrates. Among these was Bul2, an arrestin-like adaptor that is a component of the Rsp5 E3 ligase and a known substrate of Rsp5 itself (51, 52). Two other known Rsp5 substrates, the arrestins Ecm21/Art2 and Art10, also showed reduced ubiquitylation in *tul1*Δ cells, suggesting that Tul1 is required for Rsp5 E3 ligase activity. This hypothesis will be tested in future studies.

The analysis rested on the assumption that individual protein levels were equivalent in wild-type and *tul1*Δ cells. To test this assumption, we performed quantitative proteomics using SILAC and compared protein expression in wild-type and *tul1*Δ cells. We found that 4.5% (53/1172) of quantified proteins were differentially expressed between wild-type and *tul1*Δ cells (H/L $\geq$ 2.0 or H/L $\leq$ 0.5, supplemental Tables S6 and S8), indicating that Tul1 is required to maintain cellular protein homeostasis. Given this finding, we corrected the ubiquitylation site data, taking into account differences in total protein levels (supplemental Table S9). Using this approach, we identified 16 additional Tul1-dependent ubiquitylation sites in 11 different proteins (supplemental Table S10). Thus, correcting for total protein expression increased the number of candidate Tul1 substrates identified. Overall, our quantitative diGly proteomics methodology identified multiple candidate substrates for the Golgi Tul1 E3 ligase. Future *in vitro* validation studies will be required in order to demonstrate that these are direct substrates.

The Dsc and Tul1 E3 ligases have been proposed to function in Golgi protein quality control and degradation (8, 13). Consistent with this idea, we found that Tul1 E3 ligase subunits showed negative genetic interactions with ESCRT genes in the MVB pathway that targets proteins for degradation in the vacuole (Fig. 4*B*). In addition, genes coding for the Tul1 E3 ligase are required under conditions of limiting ubiquitin caused by deletion of the deubiquitylating enzyme Doa4 (Fig. 4*C*). Interestingly, we identified several Tul1 substrates with functional links to the secretory pathway: Bul2, Akl1, Rdi1, Pal1, Ktr1, and Gga2 (Table I, supplemental Table S10), making these proteins promising substrates.

Despite employing a proteomic approach, we identified a limited number of candidate Tul1 substrates (Table I, supplemental Table S10). One possible explanation is that Tul1 substrates are rapidly degraded, and we quantified ubiquitylation in the absence of proteasome inhibitors. During method optimization, we observed that proteasome inhibition caused the accumulation of polyubiquitin chains, and the resultant high level of ubiquitylation sites on ubiquitin prevented the detection of novel sites (data not shown). Alternatively, if the Tul1 E3 ligase functions in protein quality control, we would expect only a small fraction of protein molecules to be ubiquitylated and degraded at any given moment. Thus, signals for these proteins may be low, and total protein levels may change little in *tul1*Δ cells. Indeed, only 13 proteins increased >2-fold in *tul1*Δ cells relative to wild-type (supplemental Table S8). Lastly, we performed our analysis under non-stress conditions; cells were cultured in synthetic complete medium and harvested in exponential growth phase. Under these conditions, few substrates may be channeled to Tul1 E3 ligase for degradation. Future studies will use this methodology to screen stress conditions under which Tul1 E3 ligase is required for growth, such as in ESCRT mutants.

Acknowledgments—Data are available via ProteomeXchange with identifier PXD000918 (username: reviewer79741@ebi.ac.uk; password: vV9 × 7TRO (http://tinyurl.com/mrl842e)). We thank Nevan J. Krogan and Pedro Beltrao for sharing ubiquitylated peptide data, Junmin Peng for providing the JMP001 strain, Hugh Pelham for the Pep12D plasmid, Shan Zhao for technical assistance, and Sumana Raychaudhuri and Rocky Cheung for manuscript comments. The authors acknowledge the joint participation by the Adrienne Helis Malvin Medical Research Foundation and the Diana Helis Henry Medical Research Foundation through its direct engagement in the continuous active conduct of medical research in conjunction with the Johns Hopkins Hospital, the Johns Hopkins University School of Medicine, the Foundation's Parkinson's Disease Programs.

* Studies were supported by funding from the National Institutes of Health (HL077588, P.J.E.; HHSN268201000032C, A.P.) and TCNP Special K project (GM103520, P.J.E. and A.P.) of the High Throughput Biology Center at Johns Hopkins University School of Medicine.

S This article contains supplemental material.

‡‡ To whom correspondence should be addressed: Peter J. Espenshade, Department of Cell Biology, Johns Hopkins University School of Medicine, 725 N. Wolfe Street, Physiology 107B, Baltimore, MD 21205. Tel.: 443-287-5026, Fax: 410-502-7826, E-mail: peter.espenshade@jhmi.edu.

REFERENCES

1. Balch, W. E., Morimoto, R. I., Dillin, A., and Kelly, J. W. (2008) Adapting proteostasis for disease intervention. *Science* **319,** 916–919
2. Wolff, S., Weissman, J. S., and Dillin, A. (2014) Differential scales of protein quality control. *Cell* **157,** 52–64
3. Finley, D., Ulrich, H. D., Sommer, T., and Kaiser, P. (2012) The ubiquitin-proteasome system of *Saccharomyces cerevisiae*. *Genetics* **192,** 319–360
4. Olzmann, J. A., Kopito, R. R., and Christianson, J. C. (2013) The mammalian endoplasmic reticulum-associated degradation system. *Cold Spring Harb. Perspect. Biol.* **5,** 1–16
5. Hampton, R. Y., and Sommer, T. (2012) Finding the will and the way of ERAD substrate retrotranslocation. *Curr. Opin. Cell Biol.* **24,** 460–466
6. Brodsky, J. L. (2012) Cleaning up: ER-associated degradation to the rescue. *Cell* **151,** 1163–1167
7. Bien, C. M., and Espenshade, P. J. (2010) Sterol regulatory element binding

proteins in fungi: hypoxic transcription factors linked to pathogenesis. *Eukaryot. Cell* **9,** 352–359
8. Stewart, E. V., Nwosu, C. C., Tong, Z., Roguev, A., Cummins, T. D., Kim, D. U., Hayles, J., Park, H. O., Hoe, K. L., Powell, D. W., Krogan, N. J., and Espenshade, P. J. (2011) Yeast SREBP cleavage activation requires the Golgi Dsc E3 ligase complex. *Mol. Cell* **42,** 160–171
9. Stewart, E. V., Lloyd, S. J., Burg, J. S., Nwosu, C. C., Lintner, R. E., Daza, R., Russ, C., Ponchner, K., Nusbaum, C., and Espenshade, P. J. (2012) Yeast sterol regulatory element-binding protein (SREBP) cleavage requires Cdc48 and Dsc5, a ubiquitin regulatory X domain-containing subunit of the Golgi Dsc E3 ligase. *J. Biol. Chem.* **287,** 672–681
10. Lloyd, S. J., Raychaudhuri, S., and Espenshade, P. J. (2013) Subunit architecture of the Golgi Dsc E3 ligase required for sterol regulatory element-binding protein (SREBP) cleavage in fission yeast. *J. Biol. Chem.* **288,** 21043–21054
11. Deshaies, R. J., and Joazeiro, C. A. (2009) RING domain E3 ubiquitin ligases. *Annu. Rev. Biochem.* **78,** 399–434
12. Christianson, J. C., Olzmann, J. A., Shaler, T. A., Sowa, M. E., Bennett, E. J., Richter, C. M., Tyler, R. E., Greenblatt, E. J., Harper, J. W., and Kopito, R. R. (2012) Defining human ERAD networks through an integrative mapping strategy. *Nat. Cell Biol.* **14,** 93–105
13. Reggiori, F., and Pelham, H. R. (2002) A transmembrane ubiquitin ligase required to sort membrane proteins into multivesicular bodies. *Nat. Cell Biol.* **4,** 117–123
14. Valdez-Taubas, J., and Pelham, H. (2005) Swf1-dependent palmitoylation of the SNARE Tlg1 prevents its ubiquitination and degradation. *EMBO J.* **24,** 2524–2532
15. Mann, M. (2006) Functional and quantitative proteomics using SILAC. *Nat. Rev. Mol. Cell Biol.* **7,** 952–958
16. Ong, S. E., Blagoev, B., Kratchmarova, I., Kristensen, D. B., Steen, H., Pandey, A., and Mann, M. (2002) Stable isotope labeling by amino acids in cell culture, SILAC, as a simple and accurate approach to expression proteomics. *Mol. Cell. Proteomics* **1,** 376–386
17. Harsha, H. C., Molina, H., and Pandey, A. (2008) Quantitative proteomics using stable isotope labeling with amino acids in cell culture. *Nat. Protoc.* **3,** 505–516
18. Carrano, A. C., and Bennett, E. J. (2013) Using the ubiquitin-modified proteome to monitor protein homeostasis function. *Mol. Cell. Proteomics* **12,** 3521–3531
19. Xu, G., Paige, J. S., and Jaffrey, S. R. (2010) Global analysis of lysine ubiquitination by ubiquitin remnant immunoaffinity profiling. *Nat. Biotechnol.* **28,** 868–873
20. Kim, W., Bennett, E. J., Huttlin, E. L., Guo, A., Li, J., Possemato, A., Sowa, M. E., Rad, R., Rush, J., Comb, M. J., Harper, J. W., and Gygi, S. P. (2011) Systematic and quantitative assessment of the ubiquitin-modified proteome. *Mol. Cell* **44,** 325–340
21. Emanuele, M. J., Elia, A. E., Xu, Q., Thoma, C. R., Izhar, L., Leng, Y., Guo, A., Chen, Y. N., Rush, J., Hsu, P. W., Yen, H. C., and Elledge, S. J. (2011) Global identification of modular cullin-RING ligase substrates. *Cell* **147,** 459–474
22. Beltrao, P., Albanese, V., Kenner, L. R., Swaney, D. L., Burlingame, A., Villen, J., Lim, W. A., Fraser, J. S., Frydman, J., and Krogan, N. J. (2012) Systematic functional prioritization of protein posttranslational modifications. *Cell* **150,** 413–425
23. Swaney, D. L., Beltrao, P., Starita, L., Guo, A., Rush, J., Fields, S., Krogan, N. J., and Villen, J. (2013) Global analysis of phosphorylation and ubiquitylation cross-talk in protein degradation. *Nat. Methods* **10,** 676–682
24. Lee, K. A., Hammerle, L. P., Andrews, P. S., Stokes, M. P., Mustelin, T., Silva, J. C., Black, R. A., and Doedens, J. R. (2011) Ubiquitin ligase substrate identification through quantitative proteomics at both the protein and peptide levels. *J. Biol. Chem.* **286,** 41530–41538
25. Sarraf, S. A., Raman, M., Guarani-Pereira, V., Sowa, M. E., Huttlin, E. L., Gygi, S. P., and Harper, J. W. (2013) Landscape of the PARKIN-dependent ubiquitylome in response to mitochondrial depolarization. *Nature* **496,** 372–376
26. Wagner, S. A., Beli, P., Weinert, B. T., Nielsen, M. L., Cox, J., Mann, M., and Choudhary, C. (2011) A proteome-wide, quantitative survey of in vivo ubiquitylation sites reveals widespread regulatory roles. *Mol. Cell. Proteomics* **10,** M111.013284
27. Burke, D., Dawson, D., and Stearns, T. (2000) *Methods in Yeast Genetics*, Cold Spring Harbor Laboratory Press, Cold Spring Harbor, NY
28. Longtine, M. S., McKenzie, A., 3rd, Demarini, D. J., Shah, N. G., Wach, A., Brachat, A., Philippsen, P., and Pringle, J. R. (1998) Additional modules for versatile and economical PCR-based gene deletion and modification in *Saccharomyces cerevisiae. Yeast* **14,** 953–961
29. Xu, P., Duong, D. M., Seyfried, N. T., Cheng, D., Xie, Y., Robert, J., Rush, J., Hochstrasser, M., Finley, D., and Peng, J. (2009) Quantitative proteomics reveals the function of unconventional ubiquitin chains in proteasomal degradation. *Cell* **137,** 133–145
30. Finley, D., Sadis, S., Monia, B. P., Boucher, P., Ecker, D. J., Crooke, S. T., and Chau, V. (1994) Inhibition of proteolysis and cell cycle progression in a multiubiquitination-deficient yeast mutant. *Mol. Cell. Biol.* **14,** 5501–5509
31. Hughes, A. L., Todd, B. L., and Espenshade, P. J. (2005) SREBP pathway responds to sterols and functions as an oxygen sensor in fission yeast. *Cell* **120,** 831–842
32. Sehgal, A., Lee, C. Y., and Espenshade, P. J. (2007) SREBP controls oxygen-dependent mobilization of retrotransposons in fission yeast. *PLoS Genet.* **3,** 1389–1396
33. Guthrie, C., and Fink, G. R. (1991) *Guide to Yeast Genetics and Molecular Biology*, Academic Press, Inc., San Diego, CA
34. Na, C. H., and Peng, J. (2012) Analysis of ubiquitinated proteome by quantitative mass spectrometry. *Methods Mol. Biol.* **893,** 417–429
35. Shevchenko, A., Tomas, H., Havlis, J., Olsen, J. V., and Mann, M. (2006) In-gel digestion for mass spectrometric characterization of proteins and proteomes. *Nat. Protoc.* **1,** 2856–2860
36. Rappsilber, J., Mann, M., and Ishihama, Y. (2007) Protocol for micro-purification, enrichment, pre-fractionation and storage of peptides for proteomics using StageTips. *Nat. Protoc.* **2,** 1896–1906
37. Cox, J., and Mann, M. (2008) MaxQuant enables high peptide identification rates, individualized p.p.b.-range mass accuracies and proteome-wide protein quantification. *Nat. Biotechnol.* **26,** 1367–1372
38. Cox, J., Neuhauser, N., Michalski, A., Scheltema, R. A., Olsen, J. V., and Mann, M. (2011) Andromeda: a peptide search engine integrated into the MaxQuant environment. *J. Proteome Res.* **10,** 1794–1805
39. Vizcaino, J. A., Deutsch, E. W., Wang, R., Csordas, A., Reisinger, F., Rios, D., Dianes, J. A., Sun, Z., Farrah, T., Bandeira, N., Binz, P. A., Xenarios, I., Eisenacher, M., Mayer, G., Gatto, L., Campos, A., Chalkley, R. J., Kraus, H. J., Albar, J. P., Martinez-Bartolome, S., Apweiler, R., Omenn, G. S., Martens, L., Jones, A. R., and Hermjakob, H. (2014) ProteomeXchange provides globally coordinated proteomics data submission and dissemination. *Nat. Biotechnol.* **32,** 223–226
40. Ryan, C. J., Roguev, A., Patrick, K., Xu, J., Jahari, H., Tong, Z., Beltrao, P., Shales, M., Qu, H., Collins, S. R., Kliegman, J. I., Jiang, L., Kuo, D., Tosti, E., Kim, H. S., Edelmann, W., Keogh, M. C., Greene, D., Tang, C., Cunningham, P., Shokat, K. M., Cagney, G., Svensson, J. P., Guthrie, C., Espenshade, P. J., Ideker, T., and Krogan, N. J. (2012) Hierarchical modularity and the evolution of genetic interactomes across species. *Mol. Cell* **46,** 691–704
41. Olzmann, J. A., Richter, C. M., and Kopito, R. R. (2013) Spatial regulation of UBXD8 and p97/VCP controls ATGL-mediated lipid droplet turnover. *Proc. Natl. Acad. Sci. U.S.A.* **110,** 1345–1350
42. Greenblatt, E. J., Olzmann, J. A., and Kopito, R. R. (2011) Derlin-1 is a rhomboid pseudoprotease required for the dislocation of mutant alpha-1 antitrypsin from the endoplasmic reticulum. *Nat. Struct. Mol. Biol.* **18,** 1147–1152
43. Lemberg, M. K. (2013) Sampling the membrane: function of rhomboid-family proteins. *Trends Cell Biol.* **23,** 210–217
44. Alexandru, G., Graumann, J., Smith, G. T., Kolawa, N. J., Fang, R., and Deshaies, R. J. (2008) UBXD7 binds multiple ubiquitin ligases and implicates p97 in HIF1alpha turnover. *Cell* **134,** 804–816
45. Costanzo, M., Baryshnikova, A., Bellay, J., Kim, Y., Spear, E. D., Sevier, C. S., Ding, H., Koh, J. L., Toufighi, K., Mostafavi, S., Prinz, J., St Onge, R. P., VanderSluis, B., Makhnevych, T., Vizeacoumar, F. J., Alizadeh, S., Bahr, S., Brost, R. L., Chen, Y., Cokol, M., Deshpande, R., Li, Z., Lin, Z. Y., Liang, W., Marback, M., Paw, J., San Luis, B. J., Shuteriqi, E., Tong, A. H., van Dyk, N., Wallace, I. M., Whitney, J. A., Weirauch, M. T., Zhong, G., Zhu, H., Houry, W. A., Brudno, M., Ragibizadeh, S., Papp, B., Pal, C., Roth, F. P., Giaever, G., Nislow, C., Troyanskaya, O. G., Bussey, H., Bader, G. D., Gingras, A. C., Morris, Q. D., Kim, P. M., Kaiser, C. A., Myers, C. L., Andrews, B. J., and Boone, C. (2010) The genetic landscape of a cell. *Science* **327,** 425–431

46. Black, M. W., and Pelham, H. R. (2000) A selective transport route from Golgi to late endosomes that requires the yeast GGA proteins. *J. Cell Biol.* **151,** 587–600
47. Becherer, K. A., Rieder, S. E., Emr, S. D., and Jones, E. W. (1996) Novel syntaxin homologue, Pep12p, required for the sorting of lumenal hydrolases to the lysosome-like vacuole in yeast. *Mol. Biol. Cell* **7,** 579–594
48. Reggiori, F., Black, M. W., and Pelham, H. R. (2000) Polar transmembrane domains target proteins to the interior of the yeast vacuole. *Mol. Biol. Cell* **11,** 3737–3749
49. Henne, W. M., Buchkovich, N. J., and Emr, S. D. (2011) The ESCRT pathway. *Dev. Cell* **21,** 77–91
50. Swaminathan, S., Amerik, A. Y., and Hochstrasser, M. (1999) The Doa4 deubiquitinating enzyme is required for ubiquitin homeostasis in yeast. *Mol. Biol. Cell* **10,** 2583–2594
51. O'Donnell, A. F. (2012) The running of the Buls: control of permease trafficking by alpha-arrestins Bul1 and Bul2. *Mol. Cell. Biol.* **32,** 4506–4509
52. Merhi, A., and Andre, B. (2012) Internal amino acids promote Gap1 permease ubiquitylation via TORC1/Npr1/14–3-3-dependent control of the Bul arrestin-like adaptors. *Mol. Cell. Biol.* **32,** 4510–4522
53. Becuwe, M., Herrador, A., Haguenauer-Tsapis, R., Vincent, O., and Leon, S. (2012) Ubiquitin-mediated regulation of endocytosis by proteins of the arrestin family. *Biochem. Res. Int.* **2012,** 242764
54. Kee, Y., Munoz, W., Lyon, N., and Huibregtse, J. M. (2006) The deubiquitinating enzyme Ubp2 modulates Rsp5-dependent Lys63-linked polyubiquitin conjugates in *Saccharomyces cerevisiae. J. Biol. Chem.* **281,** 36724–36731
55. Gupta, R., Kus, B., Fladd, C., Wasmuth, J., Tonikian, R., Sidhu, S., Krogan, N. J., Parkinson, J., and Rotin, D. (2007) Ubiquitination screen using protein microarrays for comprehensive identification of Rsp5 substrates in yeast. *Mol. Syst. Biol.* **3,** 116